
DEEP k -GROUPING: AN UNSUPERVISED LEARNING FRAMEWORK FOR COMBINATORIAL OPTIMIZATION ON GRAPHS AND HYPERGRAPHS

Sen Bai

Changchun University of Science
and Technology, China
baisen@cust.edu.cn

Chunqi Yang

Changchun University of Science
and Technology, China
yangchunqi@mails.cust.edu.cn

Xin Bai

Huawei Technologies Co. Ltd
China
baixinbs@163.com

Xin Zhang

Changchun University of Science
and Technology, China
zhangxin@cust.edu.cn

Zhengang Jiang

Changchun University of Science
and Technology, China
jiangzhengang@cust.edu.cn

June 13, 2025

ABSTRACT

Along with AI computing shining in scientific discovery, its potential in the combinatorial optimization (CO) domain has also emerged in recent years. Yet, existing unsupervised neural network solvers struggle to solve k -grouping problems (e.g., coloring, partitioning) on large-scale graphs and hypergraphs, due to limited computational frameworks. In this work, we propose Deep k -grouping, an unsupervised learning-based CO framework. Specifically, we contribute: **(I)** Novel *one-hot encoded polynomial unconstrained binary optimization* (OH-PUBO), a formulation for modeling k -grouping problems on graphs and hypergraphs (e.g., graph/hypergraph coloring and partitioning); **(II)** GPU-accelerated algorithms for large-scale k -grouping CO problems. Deep k -grouping employs the relaxation of large-scale OH-PUBO objectives as differentiable loss functions and trains to optimize them in an unsupervised manner. To ensure scalability, it leverages GPU-accelerated algorithms to unify the training pipeline; **(III)** A Gini coefficient-based continuous relaxation annealing strategy to enforce discreteness of solutions while preventing convergence to local optima. Experimental results demonstrate that Deep k -grouping outperforms existing neural network solvers and classical heuristics such as SCIP and Tabu.

1 Introduction

The majority of combinatorial optimization (CO) problems are NP-hard or NP-complete, making large-scale CO instances computationally intractable. While problem-specific heuristics exist, a general approach is to formulate CO problems as integer programs (IP) and solve them with IP solvers. However, IP solvers lack scalability for large-scale CO instances. This has motivated recent research to explore end-to-end neural network solvers [1, 2, 3, 4] as a scalable alternative.

In the field of neural CO, unsupervised learning approaches [5, 6, 7, 8, 9, 10] show promising prospects. Unsupervised learning approaches eliminate the need for datasets of pre-solved problem instances. Instead, they leverage CO objectives as their loss functions, optimizing these objectives by training the machine learning models. However, neural networks typically operate in a differentiable parameter space, while CO requires discrete solution spaces.

Consequently, unsupervised neural network-based CO frameworks have two restrictions: **(i)** CO problems must be expressible in unconstrained objectives rather than IP problems composed of objectives and constraints; **(ii)** They necessitate differentiable relaxations of discrete variables. To this end, a line of unsupervised neural network

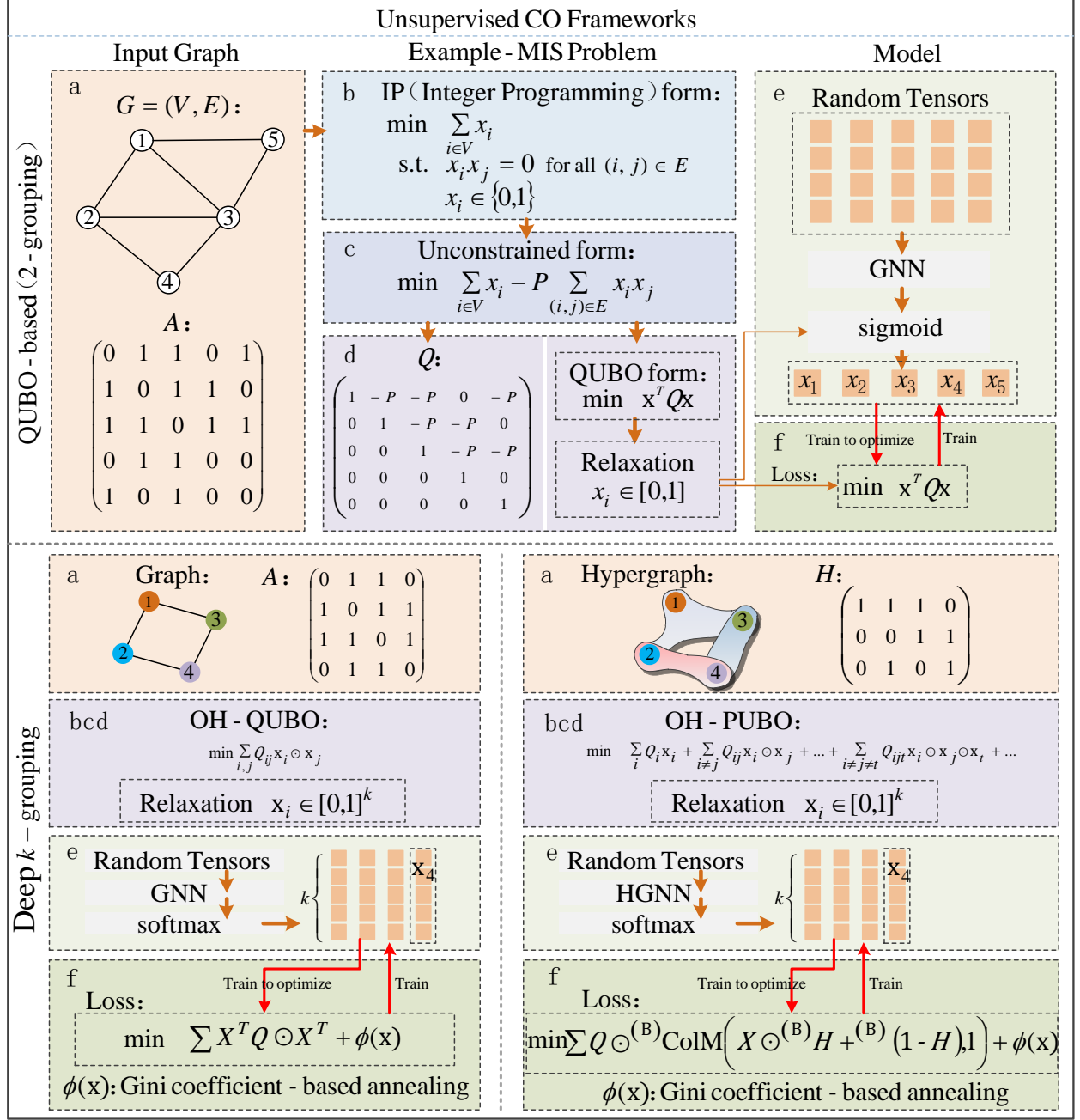


Figure 1: Overview of unsupervised neural network-based CO frameworks, including QUBO-based neural network solvers and the proposed Deep k -grouping framework.

solvers [5, 8, 9] formulate CO problems as *quadratic unconstrained binary optimization* (QUBO) problems. The QUBO problem is to optimize the following cost function:

$$\min O_{\text{QUBO}} = \sum_{i=1}^n \sum_{j=1}^n Q_{ij} x_i x_j = \mathbf{x}^T Q \mathbf{x} \quad (1)$$

where $\mathbf{x} = (x_1, x_2, \dots, x_n)$ is an n -dimensional vector of binary decision variables $x_i \in \{0, 1\}$. The QUBO matrix Q is either symmetric or in upper triangular form.

QUBO aligns with unsupervised neural CO in three aspects: (i) Unconstrained objectives. It uses penalty method [11] to incorporate constraints into the objective function; (ii) Well-suited activation functions. Sigmoid function provides a

natural mechanism for generating the relaxation of binary variables $x_i \in [0, 1]$; (iii) GPU-accelerated loss functions with uniform formulation. $\mathbf{x}^T Q \mathbf{x}$ can be efficiently computed through deep learning frameworks like PyTorch via matrix operations. The training pipeline for QUBO-based methods is illustrated in Fig. 1, incorporating a case study of the maximum independent set (MIS) problem in Appendix B.

Nevertheless, QUBO-based methods are restricted to 2-grouping problems (MIS, max-cut, etc.). When applied to k -grouping problems on graphs or hypergraphs, QUBO-based methods face challenges. **Challenge 1:** QUBO employs binary variables $x_i \in \{0, 1\}$, which are compatible with only 2-grouping tasks (such as distinguishing dominators and dominatees in the MIS problem); **Challenge 2:** Quadratic terms such as $x_i x_j$ cannot represent multi-variable correlations such as coloring conflicts within hyperedges. Thus, QUBO formulations fail to effectively model CO problems on hypergraphs. These challenges significantly limit the scalability of unsupervised CO frameworks on numerous problems, such as graph/hypergraph coloring and partitioning.

An intuitive idea to address **Challenge 1** is to employ one-hot vectors instead of binary variables. To tackle multi-variable correlations in **Challenge 2**, we generalize QUBO to *polynomial unconstrained binary optimization* (PUBO). These solutions lead us to **Challenge 3:** Is there an efficient loss function with uniform formulation for learning-based k -grouping frameworks in the way of QUBO-based approaches? To address these challenges, we present Deep k -grouping, an unsupervised neural network solver for solving CO problems. We contribute:

1) OH-QUBO/OH-PUBO Formulations. Novel *one-hot encoded quadratic (or polynomial) unconstrained binary optimization* formulations for modeling k -grouping CO problems, encoding CO objectives and constraints via Hadamard products of one-hot vectors. By leveraging the differentiable softmax relaxation of one-hot variables, Deep k -grouping enables end-to-end unsupervised optimization.

2) GPU-Accelerated Differentiable Optimization. A training pipeline enhancing the scalability of Deep k -grouping when applied to large-scale CO instances.

3) Gini Coefficient-based Annealing. A continuous relaxation annealing strategy serves a dual purpose: in the high-temperature phase, it broadly searches the solution space to escape local optima; in the low-temperature phase, it enforces the discreteness of solutions.

4) Novel Cost Functions for Graph/Hypergraph Coloring/Partitioning. An empirical study on these problems demonstrates the performance of Deep k -grouping.

Notations. For a k -grouping problem on a graph or hypergraph $G = (V, E)$, we have:

\mathbf{x}_i : the group assignment of a vertex v_i is denoted by a k -dimensional one-hot vector $\mathbf{x}_i \in \{0, 1\}^k$.

X : the group assignment matrix of all vertices $[\mathbf{x}_1, \mathbf{x}_2, \dots, \mathbf{x}_{|V|}]$ is denoted by $X \in \mathbb{R}^{|V| \times k}$.

$\sum \mathbf{x}$ or $\sum X$: the sum of all elements of a vector \mathbf{x} or a matrix X is denoted as $\sum \mathbf{x}$ or $\sum X$.

$\phi(\mathbf{x})$: the Gini coefficient-based penalty term (refer to Eq. 12, Sec. 2.4).

2 Method

Deep k -grouping (Fig. 1) solves k -grouping CO problems on graphs and hypergraphs in two stages: (i) formulating CO problems as unconstrained cost functions, including OH-QUBO or OH-PUBO (Sec. 2.1 and Sec. 2.2), and (ii) relaxing them into differentiable loss functions and training to solve them via neural network-based optimizer (Sec. 2.3 and Sec. 2.4).

2.1 Unconstrained Formulation of k -grouping CO Problems

OH-QUBO and OH-PUBO employ one-hot vectors $\mathbf{x}_i \in \{0, 1\}^k$ as decision variables to denote the group assignments. The constraints within a set of vertices are represented via Hadamard products¹ such as $\sum (\mathbf{x}_1 \odot \dots \odot \mathbf{x}_m) = \begin{cases} 1, & \text{if assigned the same group,} \\ 0, & \text{if assigned more than one group.} \end{cases}$

¹Hadamard product is denoted by \odot . For notational consistency, $\mathbf{x}_i \odot \mathbf{x}_j$ is still described as quadratic-cost terms.

Definition 1 (One-Hot Encoded QUBO or OH-QUBO). Given a graph $G = (V, E)$, the cost function of an OH-QUBO problem on G can be expressed as:

$$\min O_{\text{OH-QUBO}} = \sum_{i=1}^{|V|} \sum_{j=1}^{|V|} Q_{ij} \mathbf{x}_i \odot \mathbf{x}_j \quad (2)$$

Similar to QUBO, $\mathbf{x}_i \odot \mathbf{x}_i = \mathbf{x}_i$, thus linear terms can be omitted from Eq. 2. The OH-QUBO matrix Q is either symmetric or in upper triangular form. \square

GPU-accelerated OH-QUBO Cost Function. Eq. 2 is equivalent to:

$$O_{\text{OH-QUBO}} = \sum X^T Q \odot X^T \quad (3)$$

Proof. See Appendix D. \square

Time Complexity Analysis. For $X^T \in \mathbb{R}^{k \times |V|}$ and $Q \in \mathbb{R}^{|V| \times |V|}$, the operation $X^T Q \odot X^T$ has time complexity $O(k|V|^2)$. With GPU acceleration utilizing P cores, this reduces to $O\left(\frac{k|V|^2}{P}\right)$ under perfect parallelization.

Definition 2 (One-Hot Encoded PUBO or OH-PUBO). The cost function of OH-PUBO problems can be expressed as:

$$\min O_{\text{OH-PUBO}} = \sum_i \left(\sum_i Q_i \mathbf{x}_i + \sum_{i \neq j} Q_{ij} \mathbf{x}_i \odot \mathbf{x}_j + \sum_{i \neq j \neq t} Q_{ijt} \mathbf{x}_i \odot \mathbf{x}_j \odot \mathbf{x}_t + \dots \right) \quad (4)$$

Definition 3 (Hypergraph). A hypergraph $G = (V, E)$ is defined as a set of nodes $V = \{v_1, v_2, \dots, v_{|V|}\}$ and a set of hyperedges $E = \{e_1, e_2, \dots, e_{|E|}\}$, where each hyperedge $e_j \in E$ is a subset of V . A hypergraph G can be represented by an incidence matrix $H \in \{0, 1\}^{|V| \times |E|}$, where $H_{ij} = 1$ if $v_i \in e_j$, and $H_{ij} = 0$ otherwise. \square

In hypergraph proper coloring, polynomial terms in Eq. 4 such as $\mathbf{x}_1 \odot \mathbf{x}_2 \odot \mathbf{x}_3$ can be used to represent the color conflicts within a hyperedge $e_j = \{v_1, v_2, v_3\}$. Our idea of GPU-accelerated OH-PUBO stems from the observation of one-to-one mapping correspondence between $O_{\text{OH-PUBO}}$ in Eq. 4 and a hypergraph $G = (V, E)$, where each polynomial term in $O_{\text{OH-PUBO}}$ corresponds to a hyperedge e_j in $E = \{e_1, e_2, \dots, e_{|E|}\}$.

GPU-accelerated OH-PUBO Cost Function. Given a hypergraph $G = (V, E)$, where each hyperedge e_j of G corresponds to a (linear or polynomial) term in Eq. 4. H is the incidence matrix of G . We define the PUBO matrix $Q \in \mathbb{R}^{1 \times |E|}$ as $Q = [Q_1, Q_2, \dots, Q_{|E|}]$, where Q_j is the coefficient for each term in Eq. 4 that corresponds hyperedge e_j , thus,

$$O_{\text{OH-PUBO}} = \sum Q \odot^{(B)} \text{ColM}(X \odot^{(B)} H +^{(B)} (1 - H), 1) \quad (5)$$

where $+^{(B)}$ or $\odot^{(B)}$ denotes the element-wise addition or Hadamard product via the broadcasting mechanism. $\text{ColM}(M, 1)$ is the column-wise multiplication over the first dimension of matrix M .

Proof. See Appendix E. \square

Time Complexity Analysis. For $X \in \mathbb{R}^{|V| \times k}$, $Q \in \mathbb{R}^{1 \times |E|}$, and $H \in \mathbb{R}^{|V| \times |E|}$, the operation in Eq. 4 has time complexity $O(k|V||E|)$. GPU significantly speeds up the computation. Element-wise operations such as Hadamard product are fully parallelizable. Column-wise reduction such as sum or product over $|V|$ uses parallel reduction techniques, leading to time complexity $O(\log|V|)$. Overall, the theoretical GPU time complexity is $O(\log|V|)$ under unrealistic core counts, or otherwise utilizing P cores, the realistic GPU time can reduce to $O\left(\frac{k|V||E|}{P}\right)$.

2.2 k -grouping Problem Instances

Based on OH-QUBO and OH-PUBO, we propose novel cost functions for several k -grouping CO problems, including graph/hypergraph coloring and partitioning. Graph and hypergraph coloring have numerous applications in areas such as image segmentation [12, 13], task scheduling [14, 15, 16], and resource allocation [17, 18, 19, 20]. They refer to the assignment of minimal number of colors to vertices such that no edge or hyperedge is monochromatic.

Graph Coloring. Given a graph $G = (V, E)$, graph coloring problems can be formulated by optimizing the cost function as follows:

$$\min O_{\text{GC}} = \sum_{k=1}^{K_{\max}} y_k + \lambda_1 \sum_{(v_i, v_j) \in E} \mathbf{x}_i \odot \mathbf{x}_j + \lambda_2 \sum_{i=1}^{|V|} \sum_{k=1}^{K_{\max}} x_{ik} (1 - y_k) + \phi(\mathbf{x}) \quad (6)$$

where $\lambda_1, \lambda_2 > 0$ are penalty parameters, $\mathbf{x}_i = (x_{i1}, x_{i2}, \dots, x_{iK_{\max}})$, $\mathbf{x}_i \in \{0, 1\}^{K_{\max}}$ are one-hot vectors that represent the color assignments, variables $y_k \in \{0, 1\}$ denote whether the k -th color is used, and K_{\max} is the predefined maximum value of chromatic number. We minimize $\sum_{k=1}^{K_{\max}} y_k$ to optimize the chromatic number. Meanwhile, two types of constraints must be satisfied: (i) $\sum_{(v_i, v_j) \in E} \mathbf{x}_i \odot \mathbf{x}_j$ ensures any pair of vertices within the same edge must be assigned different colors; (ii) $\sum_{i=1}^{|V|} \sum_{k=1}^{K_{\max}} x_{ik}(1 - y_k)$ ensures that $x_{ik} \leq y_k$, thus the k -th color should not be used by any vertex if $y_k = 0$. During training, $\lambda_1 \sum_{(v_i, v_j) \in E} \mathbf{x}_i \odot \mathbf{x}_j$ can be implemented through GPU-accelerated OH-QUBO cost function in Eq. 3, where $Q_{ij} = 1$ if $(v_i, v_j) \in E$, or otherwise $Q_{ij} = 0$. Other terms in Eq. 6 can be implemented through matrix operations.

Hypergraph Strong Coloring. Given a hypergraph $G = (V, E)$, the hypergraph strong coloring problem (all vertices in any given hyperedge have distinct colors) is to optimize the cost function:

$$\min O_{\text{HSC}} = \sum_{k=1}^{K_{\max}} y_k + \lambda_1 \sum_{\substack{(v_i, v_j) \in e \\ e \in E}} \mathbf{x}_i \odot \mathbf{x}_j + \lambda_2 \sum_{i=1}^{|V|} \sum_{k=1}^{K_{\max}} x_{ik}(1 - y_k) + \phi(\mathbf{x}) \quad (7)$$

where e are hyperedges in E . Similarly, $\lambda_1 \sum_{\substack{(v_i, v_j) \in e \\ e \in E}} \mathbf{x}_i \odot \mathbf{x}_j$ can be implemented through Eq. 3, where $Q_{ij} = 1$ if $(v_i, v_j) \in e$ and $e \in E$, or otherwise $Q_{ij} = 0$.

Hypergraph Proper Coloring. Given a hypergraph $G = (V, E)$, the hypergraph proper coloring problem (no hyperedge is monochromatic) is to optimize the cost function:

$$\min O_{\text{HSC}} = \sum_{k=1}^{K_{\max}} y_k + \lambda_1 \sum_{\substack{(v_{j1}, \dots, v_{j|e|}) \in e \\ e \in E}} \mathbf{x}_{j1} \odot \dots \odot \mathbf{x}_{j|e|} + \lambda_2 \sum_{i=1}^{|V|} \sum_{k=1}^{K_{\max}} x_{ik}(1 - y_k) + \phi(\mathbf{x}) \quad (8)$$

where e are hyperedges in E . Similarly, $\lambda_1 \sum_{\substack{(v_{j1}, \dots, v_{j|e|}) \in e \\ e \in E}} \mathbf{x}_{j1} \odot \dots \odot \mathbf{x}_{j|e|}$ can be implemented through GPU-accelerated OH-PUBO cost function in (Eq. 5), where $Q_i = 1$.

Graph and hypergraph partitioning serve as building blocks in numerous applications, including VLSI design [21, 22], image segmentation [23, 24], storage sharding in distributed databases [25, 26], and simulations of distributed quantum circuits [27, 28]. They seek to partition the node set of a graph or hypergraph into multiple similarly-sized disjoint blocks while reducing the number of edges (hyperedges) that span different blocks.

Graph Partitioning. Given a graph $G = (V, E)$, the graph partitioning problem can be formulated by optimizing the following cost function:

$$\min O_{\text{GP}} = \alpha \sum_{(v_i, v_j) \in E} (\mathbf{x}_i + \mathbf{x}_j - 2\mathbf{x}_i \odot \mathbf{x}_j) + \beta \sum_{k=1}^K (|P_k| - \frac{|V|}{K})^2 + \phi(\mathbf{x}) \quad (9)$$

where $\mathbf{x}_i, \mathbf{x}_j$ are K -dimensional one-hot encoded decision vectors, α and β are hyperparameters, K is the predefined number of partitioned blocks, and $|P_k|$ denotes the number of vertices in partitioned block P_k . The OH-QUBO term $\sum (\mathbf{x}_i + \mathbf{x}_j - 2\mathbf{x}_i \odot \mathbf{x}_j)$ represents the number of cut edges. $\sum (\mathbf{x}_i + \mathbf{x}_j - 2\mathbf{x}_i \odot \mathbf{x}_j) = 0$ if \mathbf{x}_i and \mathbf{x}_j are assigned the same color, or otherwise it equals to 2. $\sum_{k=1}^K (|P_k| - \frac{|V|}{K})^2$ ensures the balancedness.

Hypergraph Partitioning. Given a hypergraph $G = (V, E)$, the hypergraph partitioning problems can be expressed as:

$$\min O_{\text{HP}} = \alpha \sum_{e_j \in E} \sum_{i=1}^{|e_j|} \frac{1}{|e_j|} (\sum_{i=1}^{|e_j|} \mathbf{x}_{ji} - |e_j| \mathbf{x}_{j1} \odot \dots \odot \mathbf{x}_{j|e_j|}) + \beta \sum_{k=1}^K (|P_k| - \frac{|V|}{K})^2 + \phi(\mathbf{x}) \quad (10)$$

where \mathbf{x}_{ji} are k -dimensional one-hot encoded decision vectors of vertices $v_{ji} \in e_j$. K is the predefined number of partitioned blocks. α and β are hyperparameters. The OH-PUBO term $\sum_{e_j \in E} \sum_{i=1}^{|e_j|} \frac{1}{|e_j|} (\sum_{i=1}^{|e_j|} \mathbf{x}_{ji} - |e_j| \mathbf{x}_{j1} \odot \dots \odot \mathbf{x}_{j|e_j|})$ represents the number of cut edges.

2.3 Neural Network-based Optimizer

Deep k -grouping solves OH-QUBO or OH-PUBO problems on graphs or hypergraphs using GNNs or hypergraph neural networks (HyperGNNs) as illustrated in Fig. 1.

Model Input: For a graph $G = (V, E)$, the GNN input consists of the adjacency matrix A and randomly initialized node features $X^{(0)} \in \mathbb{R}^{|V| \times d^{(0)}}$. For a hypergraph $G = (V, E)$, HyperGNNs take the incidence matrix H and the same randomly initialized $X^{(0)}$ as input.

Model Architecture: Typically, the neural networks combine GNN (or HyperGNN) layers with fully connected (FC) layers, with architectures intrinsically adapted to the problem. For instance, graph (hypergraph) partitioning necessitates the capture of global structural information, thereby requiring a deep GNN (or HyperGNN) model (4-8 layers) supplemented by FC layers. In contrast, the graph coloring problem emphasizes local information, thus demanding a shallow model (2-3 layers) comprised solely of GNN layers.

Model Output: The neural networks apply the softmax function to produce the relaxation of one-hot decision variables, represented as a matrix $X \in \mathbb{R}^{|V| \times k}$. The i -th row of X , denoted by $\mathbf{x}_i \in [0, 1]^k$, corresponds to the assignment probability vector of vertex v_i over k groups.

More concretely, the neural network model operates as follows:

$$X = \text{Softmax}(\text{FC}(\text{GNN}(A, X^{(0)}))) \quad \text{or} \quad X = \text{Softmax}(\text{FC}(\text{HyperGNN}(H, X^{(0)}))) \quad (11)$$

where GNN or HyperGNN is a multi-layer graph or hypergraph convolutional network.

Loss Function: The neural network-based optimizer aims to minimize the OH-QUBO or OH-PUBO objective function. To achieve this, Deep k -grouping employs the softmax-relaxation of OH-QUBO or OH-PUBO objective function as a differentiable loss function $L(X)$, with respect to X , the output of the neural network model. We aim to find the optimal solution $X^s = \text{argmin} L(X)$.

Training to Optimize: On this basis, Deep k -grouping optimizes the loss function through unsupervised training. Meanwhile, the group assignment matrix X will converge to approximate solutions X^s of OH-QUBO or OH-PUBO problems.

2.4 Gini Coefficient-based Annealing

Neural network-based unsupervised CO solvers face two issues: **(i)** Neural networks are prone to getting stuck in local optima; **(ii)** The differentiable relaxation of discrete decision variables leads to soft solutions of continuous values. To address these issues, CRA-PI-GNN [8] introduces a continuous relaxation annealing strategy. It leverages the penalty term $\gamma \sum_{i=1}^n (1 - (2x_i - 1)^\alpha)$ to avoid local optima and enforce the discreteness of solutions, where $x_i \in [0, 1]$ are relaxed variables, γ controls the penalty strength and α is an even integer.

Inspired by CRA-PI-GNN, we explore the continuous relaxation annealing strategy for the softmax relaxation of one-hot variables $\mathbf{x}_i \in [0, 1]^k$. Let $\mathbf{x}_i = (x_{i1}, x_{i2}, \dots, x_{ik})$ be a probability vector, where $\sum_{j=1}^k x_{ij} = 1$ and $x_{ij} \geq 0$. An intuitive approach is to use Shannon entropy [29] term $\gamma \sum_{i=1}^n \sum_{j=1}^k -x_{ij} \log x_{ij}$ as the penalty. However, Shannon entropy function is infeasible for neural networks since the gradient diverges to $\pm\infty$ at 0 or 1. To address this issue, we need to find an alternative function that exhibits the same trend of variation as the Shannon entropy. To this end, we employ Gini coefficient-based penalty term:

$$\phi(\mathbf{x}) = \gamma \sum_{i=1}^n \left(1 - \sum_{j=1}^k x_{ij}^2 \right) \quad (12)$$

For a one-hot vector \mathbf{x}_i , the value of Gini coefficient $1 - \sum_{j=1}^k x_{ij}^2 = 0$, or otherwise when \mathbf{x}_i is uniform ($x_{ij} = \frac{1}{k}$), the maximum value of Gini coefficient is $1 - \frac{1}{k}$. The annealing strategy enhances the learning process by gradually annealing the parameter γ : **(i)** Initially, γ is set to a negative value ($\gamma < 0$) to smooth the model, thereby facilitating broad search of the solution space and avoiding local optima; **(ii)** Subsequently, the value of γ is gradually increased (until $\gamma > 0$) to enforce the discreteness of solutions.

3 Experiments

Datasets and Baseline Methods. We evaluate the performance of Deep k -grouping on synthetic and real-world graph and hypergraph datasets (refer to Tab. 4 in Appendix F). Baseline methods include **(i)** IP solvers (e.g., SCIP [30] and Tabu [31]); **(ii)** Neural network solvers (e.g., GAP [6] for graph partitioning); **(iii)** Problem-specific heuristics (e.g., hMETIS [21] and KaHyPar [32] for graph/hypergraph partitioning).

Implementation. The GPU used in the experiment is an NVIDIA GeForce RTX 3090 with 24 G of memory. We implement GNNs and HyperGNNs with DHG library [33, 34].

Table 1: Experimental Results for Graph Coloring.

Method	BAT	EAT	UAT	DBLP	CiteSeer	AmzPhoto	AmzPc
SCIP	18 (2 s)	29 (9 s)	64 (25 s)	8 (16 s)	8 (22 s)	-	-
	16 (16 s)	25 (12 s)	60 (32 s)	7 (37 s)	7 (66 s)	-	-
Tabu	25 (17 s)	53 (59 s)	79 (898 s)	12 (123 s)	15 (195 s)	146 (2,770 s)	-
Ours	18 (2 s)	29 (2 s)	65 (8 s)	7 (4 s)	7 (20 s)	48 (90 s)	52 (263 s)

Table 2: Experimental Results for Hypergraph Proper Coloring.

Method	Primary	High	Cora	PubMed	Cooking200
SCIP	29 (12 s)	20 (424 s)	4 (13 s)	5 (15 s)	3 (36 s)
	27 (557 s)	20 (424 s)	3 (30 s)	4 (27 s)	2 (851 s)
Tabu	41 (3,378 s)	26 (2,124 s)	5 (102 s)	7 (254 s)	4 (1,654 s)
Ours	35 (5 s)	20 (6 s)	4 (8 s)	5 (7 s)	3 (6 s)

3.1 Graph/Hypergraph Coloring

We use real-world datasets (Tab. 1 and Tab. 2) to evaluate the performance of Deep k -grouping on graph coloring and hypergraph proper coloring. We use 2-layer GraphSAGE [35] as the learning model, since various GNNs and HyperGNNs have been examined and GraphSAGE always achieves the best performance on either graphs or hypergraphs. To adapt GraphSAGE for vertex embedding tasks in hypergraph proper coloring, the hypergraphs are transformed into graphs through clique expansion. We apply max pooling to generate decision variables for colors $\mathbf{y} = (y_1, \dots, y_{K_{max}})$ in Eq. 6 or Eq. 8 as follows: $\mathbf{y} = \text{Sigmoid}(\text{MP}(\text{GraphSAGE}(A, X^{(0)})))$, where MP is the max pooling layer. The values of penalty parameters λ_1, λ_2 are initialized to 0 and gradually increased during training to satisfy the constraints. The learning rate η is set to 1^{-4} .

As depicted in Tab. 1 and Tab. 2, the chromatic number and the initial time to find a corresponding solution (e.g., 18 (2 s)) are depicted in the tables. SCIP outperforms Deep k -grouping and Tabu on small datasets such as BAT, EAT, and UAT. However, we ran SCIP on large-scale datasets including AmzPc and AmzPhoto for 5 hours but cannot find any feasible solution. That is, Deep k -grouping achieves superior performance to SCIP and Tabu for large-scale graph coloring problems. For hypergraph proper coloring, we observe that while Deep k -coloring can color hypergraphs faster, yet it struggles to find the optimal chromatic number as SCIP does. Notably, SCIP’s significant performance is achieved through novel objective functions we proposed in Sec. 2.2.

3.2 Graph/Hypergraph Partitioning

We evaluate the performance of Deep k -grouping on graph/hypergraph partitioning as depicted in Tab. 3. Best performed GAT [36] with 2 or 3 layers is applied to construct Deep k -grouping for graph partitioning. For hypergraph partitioning, Deep k -grouping achieves best solutions with 4 ~ 8-layer HGNN+ [33] incorporating FC layers. $\frac{\alpha}{\beta}$ is assigned a fixed value and the learning rate η is set to 1^{-4} . The runtime of SCIP was limited to 1 hour. As the evaluation results shown in Tab. 3, on small datasets, SCIP can find the optimal solution. However, as the data scale and the value of k increase, the solution space grows exponentially, making it challenging for SCIP to approximate the optimal solution. In such scenarios, Deep k -grouping outperforms other methods.

3.3 Runtime Comparison with SCIP

We conduct additional experiments to comprehensively evaluate the solving time differences between Deep k -grouping and SCIP. The single-objective max-cut problem on graphs (refer to Appendix C) is adopted to exclude the effects of extraneous optimization objectives such as balancedness.

The runtime of SCIP and Deep k -grouping has been tested when vertex counts $|V|$ of graphs $G = (V, E)$ are ranging from 40 to 110, and $|E| = 4|V|$. SCIP was terminated immediately when it found a feasible solution. We trained Deep k -grouping until it converged. As illustrated in Fig. 2, Deep k -grouping’s runtime remains stable while SCIP’s runtime grows exponentially with graph size. This further explains why Deep k -grouping achieves better performance on large-scale datasets.

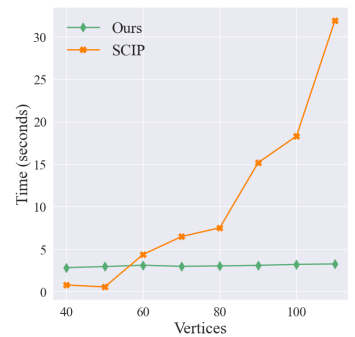
Figure 2: Comparison of the runtime between SCIP and Deep k -grouping.

Table 3: Performance comparison of graph/hypergraph partitioning methods including Deep k -grouping, GAP (neural network-based), hMETIS, and KaHyPar (problem-specific multi-level heuristics). BAT, EAT, UAT, DBLP, CiteSeer are graphs. Primary, High, Cora, PubMed, and Cooking200 are hypergraphs. Three metrics— C (B_1, B_2) have been illustrated in the table, where C is the number of cut edges, $B_1 = \frac{\max(S)}{\min(S)} - 1$ and $B_2 = \sqrt{\frac{1}{k} \sum_{i=1}^k (|P_i| - \text{mean}(S))^2}$ are two types of balancedness (the smaller the value of B_1 and B_2 , the better the balancedness), and $S = \{|P_1|, |P_2|, \dots, |P_k|\}$ is the set of partition block sizes.

Dataset	Method	$k = 2$	$k = 3$	$k = 4$	$k = 5$	$k = 6$
BAT	hMETIS	192 (2.3%,1.5)	368 (5.3%,2.1)	465 (6.9%,2.3)	528 (11%,1.9)	593 (9.9%,1.3)
	GAP	192 (2.3%,1.5)	362 (5.3%,1.7)	456 (6.9%,1.3)	526 (6.9%,1.0)	569 (9.9%,1.1)
	SCIP	198 (0%,0)	369 (0%,0)	491 (0%,0)	556 (0%,0)	589 (0%,0)
	Ours	191 (2.3%,1.5)	346 (5.3%,1.7)	446 (6.9%,1.3)	514 (6.9%,1.2)	567 (9.9%,1.1)
EAT	hMETIS	946 (2.3%,4.5)	2,034 (3.8%,3.6)	2,565 (5.3%,5.3)	2,990 (6.5%,4.5)	2,983 (46%,22)
	GAP	946 (2.3%,4.5)	2,047 (3.8%,3.6)	2,626 (6.3%,3.7)	2,917 (6.5%,3.5)	2,913 (50%,15)
	SCIP	996 (0%,0)	2,224 (0%,0)	3,065 (0%,0)	3,863 (0%,0)	4,965 (0%,0)
	Ours	946 (2.3%,4.5)	2,015 (3.8%,3.6)	2,554 (5.3%,3.9)	2,915 (6.5%,3.2)	2,871 (43%,13)
UAT	hMETIS	411 (2.0%,12)	1,078 (3.9%,11)	1,783 (4.2%,9.0)	2,568 (5.5%,11)	2,877 (46%,61)
	GAP	410 (2.2%,13)	1,138 (4.1%,12)	1,842 (3.2%,5.5)	2,585 (5.0%,6.0)	2,820 (21%,18)
	SCIP	424 (0%,0)	1,488 (0%,0)	2,643 (0%,0)	8,997 (0%,0)	11,159 (0%,0)
	Ours	407 (2.0%,12)	1,076 (3.9%,11)	1,755 (3.2%,5.5)	2,499 (4.6%,5.5)	2,719 (20%,18)
DBLP	hMETIS	84 (0%,0)	136 (0%,0)	166 (0%,0)	186 (0%,0)	223 (0%,0)
	GAP	198 (0%,0)	322 (0%,0)	332 (0%,0)	432 (0.2%,0.7)	399 (8.6%,19)
	SCIP	38 (0%,0)	83 (0%,0)	222 (0%,0)	1,248 (0%,0)	515 (0%,0)
	Ours	74 (0%,0)	113 (0%,0)	156 (0%,0)	168 (0%,0)	213 (0.8%,2.5)
CiteSeer	hMETIS	27 (0%,0)	70 (0%,0)	101 (0.2%,0.8)	145 (0%,0)	152 (0%,0)
	GAP	193 (0%,0)	430 (0%,0)	426 (0.2%,0.8)	440 (0.3%,1.7)	536 (0%,0)
	SCIP	25 (0%,0)	27 (0%,0)	49 (0%,0)	140 (0%,0)	1258 (0%,0)
	Ours	39 (0%,0)	62 (0%,0)	93 (0%,0)	118 (0%,0)	142 (0.3%,0.8)
Primary	KaHyPar	2,582 (0.8%,1)	4,070 (0%,0)	5,072 (0%,0)	5,190 (0%,0)	6,576 (0%,0)
	SCIP	3,614 (0%,0)	7,792 (0%,0)	8,758 (0%,0)	11,323 (0%,0)	11,420 (0%,0)
	Ours	2,582 (0.8%,1)	4,070 (0%,0)	5,072 (0%,0)	5,181 (0%,0)	6,484 (0%,0)
High	KaHyPar	793 (1.0%,2.5)	828 (1.0%,0.8)	1,530 (0%,0)	1,916 (0%,0)	2,151 (0%,0)
	SCIP	905 (0%,0)	1,520 (0%,0)	6,127 (0%,0)	6,389 (0%,0)	6,558 (0%,0)
	Ours	784 (1.5%,2.5)	812 (2.8%,2.2)	1,523 (0%,0)	1,903 (0%,0)	2,149 (0%,0)
Cora	KaHyPar	123 (0%,0)	172 (0.4%,1.7)	201 (0%,0)	237 (0.8%,2.6)	270 (0.6%,2.2)
	SCIP	116 (0%,0)	151 (0%,0)	210 (0%,0)	232 (0%,0)	324 (0%,0)
	Ours	122 (0%,0)	169 (0%,0)	200 (0%,0)	234 (0%,0)	261 (0%,0)
PubMed	KaHyPar	814 (0%,0)	1,253 (0%,0)	1,476 (0.6%,9.3)	1,864 (0.9%,12)	2,083 (1.1%, 15)
	SCIP	911 (0%,0)	5,463 (0%,0)	6,388 (0%,0)	5,887 (0%,0)	-
	Ours	844 (0%,0)	1,157 (0%,0)	1,455 (0.3%,3.1)	1,855 (0.8%,9.5)	2,048 (0%,0)
Cooking 200	KaHyPar	1,093 (0%,0)	1,304 (0%,0)	1,454 (0%,0)	1,507 (0%,1.5)	1,560 (0.7%,7.9)
	SCIP	1,073 (0%,0)	1,978 (0%,0)	2,395 (0%,0)	2,022 (0%,0)	2,036 (0%,0)
	Ours	1,283 (0%,0)	1,305 (0%,0)	1,406 (0%,0)	1,439 (0%,0.8)	1,511 (0%,0)

3.4 Ablation Study on the Annealing Strategy

We validate the effectiveness of Deep k -grouping with or without Gini coefficient-based annealing strategy.

As illustrated in Fig. 3, we first evaluated the quality of solutions of the max-cut problem across different graph scales. The experiments tested the performance of the Gini coefficient-based annealing strategy on graphs with 2,000 \sim 3,000 vertices, generating 50 random graphs (where $|V| = |E|$) each time and averaging the cut numbers. Experimental results in Fig. 3 demonstrate that the Gini coefficient-based annealing strategy effectively enhances solution quality, demonstrating its ability to prevent the model from getting trapped in local optima.

We also conducted experiments to verify that Gini coefficient-based annealing enforces the discreteness of solutions. The experiments were conducted on a graph with 5,000 vertices and 5,000 edges. It measured the quality of solutions and their convergence behavior on the max-cut problem with increasing training epochs. Initially, the penalty strength γ was set to -2.5 and gradually increased its value during training. It reached 0 after 1000 epochs and continued to increase thereafter. As shown in Fig. 4, the Gini coefficient-based annealing strategy ensures sustained acquisition of higher-quality solutions while guaranteeing complete convergence to discrete values. In contrast, when this annealing strategy is disabled, a growing proportion of nodes exhibit failed convergence to discrete solutions as training epochs increase.

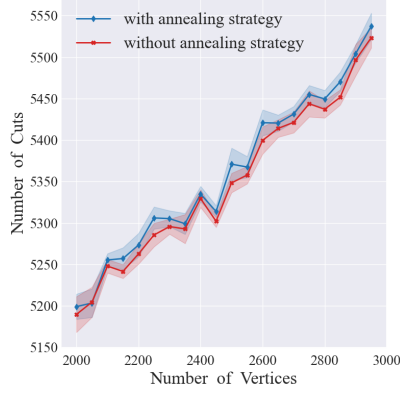


Figure 3: Quality of solutions of the max-cut problem with or without Gini coefficient-based annealing strategy across various graph sizes.

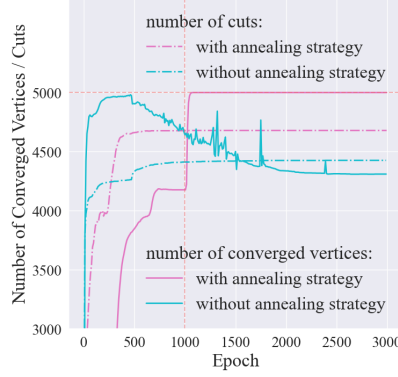


Figure 4: Quality and discreteness of solutions of the max-cut problem with or without Gini coefficient-based annealing strategy.

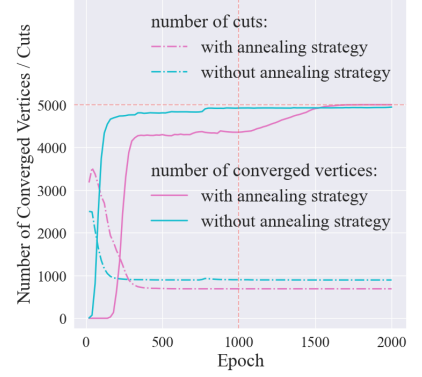


Figure 5: Quality and discreteness of solutions of the graph partitioning problem with or without Gini coefficient-based annealing strategy.

We further evaluated the Gini coefficient-based annealing strategy for the graph partitioning problem ($k = 4$). The experiments were conducted on a graph comprising 5,000 vertices and 5,000 edges. The penalty strength γ was set to -0.25 and reached 0 after 1000 epochs and continued to increase thereafter. We monitored the cut number and discreteness of solutions with increasing training epochs. As illustrated in Fig. 5, negative γ values enable the model to escape local optima, thereby discovering higher-quality solutions. Conversely, positive γ guarantees convergence of all vertices states to discrete assignments, which rigorously enforces the constraints. Conversely, when parameter γ is set to positive values, the system exhibits accelerated convergence dynamics, where all variables rigorously converge to discrete states eventually.

4 Conclusions

In this work, we propose Deep k -grouping, an unsupervised neural network solver for solving k -grouping CO problems on graphs and hypergraphs.

Algorithm Design. We propose OH-QUBO and OH-PUBO formalisms for modeling k -grouping CO problems. On this basis, we propose a GPU-accelerated and Gini coefficient-based annealing enhanced training pipeline to solve k -grouping CO problems in an end-to-end manner.

Extensive Experiments & Empirical Findings. We propose novel cost functions for graph/hypergraph coloring/partitioning problems. Although exact solvers like SCIP can exhaustively search for globally optimal solutions for small-scale datasets, experimental results have demonstrated the performance of Deep k -grouping on large-scale optimization problems. Deep k -grouping outperforms existing approximate solvers, including neural network solvers and problem-specific heuristics. Neural solvers such as Deep k -grouping establish new state-of-the-art performance and hold promise in tackling real-world CO challenges.

References

- [1] Huigen Ye, Hua Xu, Hongyan Wang, Chengming Wang, and Yu Jiang. Gnn&gbdt-guided fast optimizing framework for large-scale integer programming. In *International conference on machine learning (ICML)*, pages 39864–39878. PMLR, 2023.
- [2] Ye Tian, Luchen Wang, Shangshang Yang, Jinliang Ding, Yaochu Jin, and Xingyi Zhang. Neural network-based dimensionality reduction for large-scale binary optimization with millions of variables. *IEEE Transactions on Evolutionary Computation*, 2024.
- [3] Qian Li, Tian Ding, Linxin Yang, Minghui Ouyang, Qingjiang Shi, and Ruoyu Sun. On the power of small-size graph neural networks for linear programming. In *The Thirty-eighth Annual Conference on Neural Information Processing Systems (NeurIPS)*, 2024.

- [4] Quentin Cappart, Didier Chételat, Elias B Khalil, Andrea Lodi, Christopher Morris, and Petar Veličković. Combinatorial optimization and reasoning with graph neural networks. *Journal of Machine Learning Research*, 24(130):1–61, 2023.
- [5] Martin JA Schuetz, J Kyle Brubaker, and Helmut G Katzgraber. Combinatorial optimization with physics-inspired graph neural networks. *Nature Machine Intelligence*, 4(4):367–377, 2022.
- [6] Azade Nazi, Will Hang, Anna Goldie, Sujith Ravi, and Azalia Mirhoseini. A deep learning framework for graph partitioning. *International Conference on Learning Representations (ICLR)*, 2019.
- [7] Anton Tsitsulin, John Palowitch, Bryan Perozzi, and Emmanuel Müller. Graph clustering with graph neural networks. *Journal of Machine Learning Research*, 24(127):1–21, 2023.
- [8] Yuma Ichikawa. Controlling continuous relaxation for combinatorial optimization. *Advances in Neural Information Processing Systems (NeurIPS)*, 37:47189–47216, 2024.
- [9] Ming Chen, Jie Chun, Shang Xiang, Luona Wei, Yonghao Du, Qian Wan, Yuning Chen, and Yingwu Chen. Learning to solve quadratic unconstrained binary optimization in a classification way. *Advances in Neural Information Processing Systems (NeurIPS)*, 37:114478–114509, 2024.
- [10] Runzhong Wang, Junchi Yan, and Xiaokang Yang. Neural graph matching network: Learning lawler’s quadratic assignment problem with extension to hypergraph and multiple-graph matching. *IEEE Transactions on Pattern Analysis and Machine Intelligence*, 44(9):5261–5279, 2021.
- [11] Fred Glover, Gary Kochenberger, Rick Hennig, and Yu Du. Quantum bridge analytics i: a tutorial on formulating and using qubo models. *Annals of Operations Research*, 314(1):141–183, 2022.
- [12] Tran Anh Tuan, Nguyen Tuan Khoa, Tran Minh Quan, and Won-Ki Jeong. Colorrl: reinforced coloring for end-to-end instance segmentation. In *Proceedings of the IEEE/CVF Conference on Computer Vision and Pattern Recognition (CVPR)*, pages 16727–16736, 2021.
- [13] D Gómez, Javier Montero, Javier Yáñez, and C Poidomani. A graph coloring approach for image segmentation. *Omega*, 35(2):173–183, 2007.
- [14] Tobias Stollenwerk, Stuart Hadfield, and Zhihui Wang. Toward quantum gate-model heuristics for real-world planning problems. *IEEE Transactions on Quantum Engineering*, 1:1–16, 2020.
- [15] Lamis R Darwish, Mohamed T El-Wakad, and Mahmoud M Farag. Towards sustainable industry 4.0: A green real-time iiot multitask scheduling architecture for distributed 3d printing services. *Journal of Manufacturing Systems*, 61:196–209, 2021.
- [16] Runa Ganguli and Siddhartha Roy. A study on course timetable scheduling using graph coloring approach. *International Journal of Computational and Applied Mathematics*, 12(2):469–485, 2017.
- [17] Kai-Ju Wu, Y-W Peter Hong, and Jang-Ping Sheu. Coloring-based channel allocation for multiple coexisting wireless body area networks: A game-theoretic approach. *IEEE Transactions on Mobile Computing*, 21(1):63–75, 2020.
- [18] Jie Huang, Shilong Zhang, Fan Yang, Tao Yu, LV Narasimha Prasad, Manisha Guduri, and Keping Yu. Hypergraph-based interference avoidance resource management in customer-centric communication for intelligent cyber-physical transportation systems. *IEEE Transactions on Consumer Electronics*, 2023.
- [19] Bowen Wang, Yanjing Sun, Zhi Sun, Long D Nguyen, and Trung Q Duong. Uav-assisted emergency communications in social iot: A dynamic hypergraph coloring approach. *IEEE Internet of Things Journal*, 7(8):7663–7677, 2020.
- [20] Sayan Mukherjee. A grover search-based algorithm for the list coloring problem. *IEEE Transactions on Quantum Engineering*, 3:1–8, 2022.
- [21] George Karypis, Rajat Aggarwal, Vipin Kumar, and Shashi Shekhar. Multilevel hypergraph partitioning: Application in vlsi domain. In *Proceedings of the 34th annual Design Automation Conference (DAC)*, pages 526–529, 1997.
- [22] Benzheng Li, Shunyang Bi, Hailong You, Zhongdong Qi, Guangxin Guo, Richard Sun, and Yuming Zhang. Mapart: an efficient multi-fpga system-aware hypergraph partitioning framework. *IEEE Transactions on Computer-Aided Design of Integrated Circuits and Systems*, 2024.
- [23] Vitor Gomes, Pablo Barcellos, and Jacob Scharcanski. Stochastic shadow detection using a hypergraph partitioning approach. *Pattern Recognition*, 63:30–44, 2017.

- [24] Shurong Chai, Rahul K Jain, Shaocong Mo, Jiaqing Liu, Yulin Yang, Yinhao Li, Tomoko Tateyama, Lanfen Lin, and Yen-Wei Chen. A novel adaptive hypergraph neural network for enhancing medical image segmentation. In *International Conference on Medical Image Computing and Computer-Assisted Intervention (MICCAI)*, pages 23–33. Springer, 2024.
- [25] Igor Kabiljo, Brian Karrer, Mayank Pundir, Sergey Pupyrev, and Alon Shalita. Social hash partitioner: a scalable distributed hypergraph partitioner. *Proceedings of the VLDB Endowment*, 10(11):1418–1429, 2017.
- [26] Wenying Yang, Guojun Wang, Kim-Kwang Raymond Choo, and Shuhong Chen. Hepart: A balanced hypergraph partitioning algorithm for big data applications. *Future Generation Computer Systems*, 83:250–268, 2018.
- [27] Pablo Andres-Martinez and Chris Heunen. Automated distribution of quantum circuits via hypergraph partitioning. *Physical Review A*, 100(3):032308, 2019.
- [28] Johnnie Gray and Stefanos Kourtis. Hyper-optimized tensor network contraction. *Quantum*, 5:410, 2021.
- [29] Gabriel Pereyra, George Tucker, Jan Chorowski, Łukasz Kaiser, and Geoffrey Hinton. Regularizing neural networks by penalizing confident output distributions. *arXiv preprint arXiv:1701.06548*, 2017.
- [30] Stephen Maher, Matthias Miltenberger, João Pedro Pedroso, Daniel Rehfeldt, Robert Schwarz, and Felipe Serrano. PySCIPOpt: Mathematical programming in python with the SCIP optimization suite. In *Mathematical Software – ICMS 2016*, pages 301–307. Springer International Publishing, 2016.
- [31] Fred Glover and Manuel Laguna. *Tabu search*. Springer, 1998.
- [32] Lars Gottesbüren, Tobias Heuer, Nikolai Maas, Peter Sanders, and Sebastian Schlag. Scalable high-quality hypergraph partitioning. *ACM Transactions on Algorithms*, 20(1):1–54, 2024.
- [33] Yue Gao, Yifan Feng, Shuyi Ji, and Rongrong Ji. Hgnn+: General hypergraph neural networks. *IEEE Transactions on Pattern Analysis and Machine Intelligence*, 45(3):3181–3199, 2022.
- [34] Yifan Feng, Haoxuan You, Zizhao Zhang, Rongrong Ji, and Yue Gao. Hypergraph neural networks. In *the AAAI Conference on Artificial Intelligence (AAAI)*, volume 33, pages 3558–3565, 2019.
- [35] Will Hamilton, Zhitao Ying, and Jure Leskovec. Inductive representation learning on large graphs. *Advances in Neural Information Processing Systems (NeurIPS)*, 30, 2017.
- [36] Petar Veličković, Guillem Cucurull, Arantxa Casanova, Adriana Romero, Pietro Liò, and Yoshua Bengio. Graph attention networks. In *International Conference on Learning Representations (ICLR)*, 2018.
- [37] Yu Xie, Lianhang Luo, Tianpei Cao, Bin Yu, and AK Qin. Contrastive learning network for unsupervised graph matching. *IEEE Transactions on Circuits and Systems for Video Technology*, 2024.
- [38] Yixiao Zhou, Ruiqi Jia, Hongxiang Lin, Hefeng Quan, Yumeng Zhao, and Xiaoqing Lyu. Improving graph matching with positional reconstruction encoder-decoder network. *Advances in Neural Information Processing Systems (NeurIPS)*, 36:34557–34569, 2023.
- [39] Siddharth Tourani, Muhammad Haris Khan, Carsten Rother, and Bogdan Savchynskyy. Discrete cycle-consistency based unsupervised deep graph matching. In *Proceedings of the AAAI Conference on Artificial Intelligence (AAAI)*, volume 38, pages 5252–5260, 2024.
- [40] Ismail Bustany, Andrew B Kahng, Ioannis Koutis, Bodhisatta Pramanik, and Zhiang Wang. Specpart: A supervised spectral framework for hypergraph partitioning solution improvement. In *the 41st IEEE/ACM International Conference on Computer-Aided Design (ICCAD)*, pages 1–9, 2022.
- [41] Ismail Bustany, Andrew B Kahng, Ioannis Koutis, Bodhisatta Pramanik, and Zhiang Wang. K-specpart: Supervised embedding algorithms and cut overlay for improved hypergraph partitioning. *IEEE Transactions on Computer-Aided Design of Integrated Circuits and Systems*, 2023.
- [42] Justin Sybrandt, Ruslan Shaydulin, and Ilya Safro. Hypergraph partitioning with embeddings. *IEEE Transactions on Knowledge & Data Engineering*, 34(06):2771–2782, 2022.

A Related works

PI-GNN [5] introduced the QUBO formulation from quantum computing into unsupervised neural CO. Building upon PI-GNN, a series of enhanced methods have been proposed, such as value classification network (VCN) [9] and continuous relaxation annealing (CRA) [8]. While these advancements demonstrate the potential of unsupervised learning in CO, prior studies primarily validated them on basic CO problems, such as MIS and max-cut.

Researchers have also formulated graph matching [10] as the quadratic assignment problem (QAP, a classic QUBO problem) and addressed it through unsupervised neural networks. Owing to its critical applications in computer vision, graph matching has been extensively investigated [37, 38, 39]. In the field of k -grouping CO, GNN-based unsupervised learning models include GAP [6] and Deep Modularity Networks (DMN) [7] for graph partitioning and clustering. Most of these neural solvers are problem-specific.

In summary, prior methods primarily focus on CO problems with either binary variables for 2-grouping problems or quadratic-cost CO problems on graphs. In this work, we extend unsupervised CO frameworks to industrially critical yet underexplored problems, such as hypergraph partitioning [40, 41, 42]—a key challenge in VLSI design and distributed computing.

B The MIS problem

The MIS problem for an ordinary graph $G = (V, E)$ can be formulated by counting the number of marked (colored by 1) vertices belonging to the independent set and adding a penalty when two vertices are connected by an edge.

IP Form. Given a graph $G = (V, E)$, the MIS problem can be formulated as the following IP form:

$$\min \quad - \sum_{i \in V} x_i \quad (13)$$

$$\text{s.t.} \quad x_i x_j = 0 \quad \text{for all } (i, j) \in E \quad (14)$$

$$x_i \in \{0, 1\} \quad (15)$$

QUBO Form. The MIS problem can be formulated as the QUBO form by using penalty method:

$$\min \quad - \sum_{i \in V} x_i + P \sum_{(i,j) \in E} x_i x_j \quad (16)$$

where P is the penalty parameter and $x_i \in \{0, 1\}$. $P > 0$ enforces the constraint that x_i and x_j cannot both be equal to 1 simultaneously.

Unsupervised Neural Network-based Optimizer. As illustrated in Fig. 1, initially, the MIS problem is phrased

in QUBO form by constructing the matrix $Q = \begin{cases} P & \text{if } (i, j) \in E \\ -1 & \text{if } i = j \\ 0 & \text{otherwise (feasible)} \end{cases}$. Subsequently, the random parameter

vectors are then fed into graph neural networks (GNN) as node features, while relaxed decision variables $x_i \in [0, 1]$ are generated through sigmoid function. Through training to minimize the loss function $\mathbf{x}^T Q \mathbf{x}$, decision variables x_i will eventually converge to solutions that are close to discrete values $\{0, 1\}$.

C The max-cut problem

The max-cut problem of a graph $G = (V, E)$ involves partitioning the vertex set into two disjoint subsets such that the number of edges crossing the partitioned blocks is maximized.

QUBO Form. The max-cut problem can be formulated as the QUBO form:

$$\min \quad \sum_{(i,j) \in E} (2x_i x_j - x_i - x_j) \quad (17)$$

where $x_i \in \{0, 1\}$.

OH-QUBO Form. The max-cut problem can be formulated as the OH-QUBO form:

$$\min \quad \sum X^T Q \odot X^T \quad (18)$$

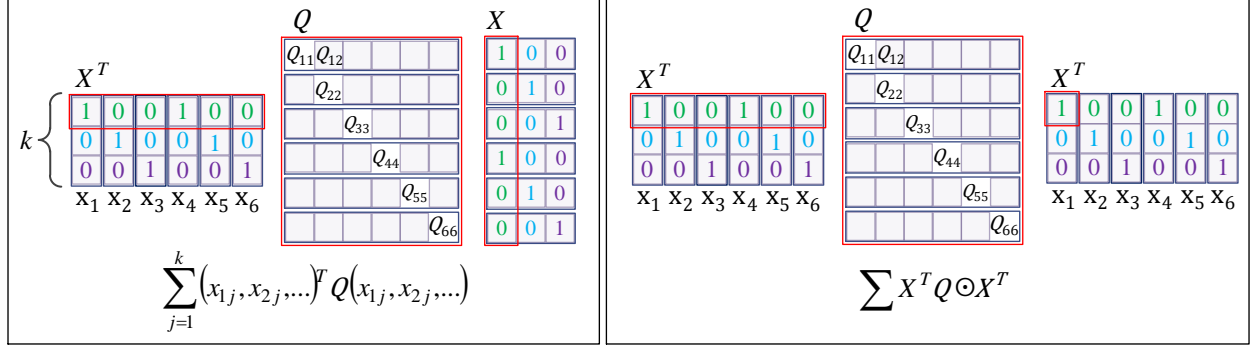


Figure 6: On the proof of Eq. 3.

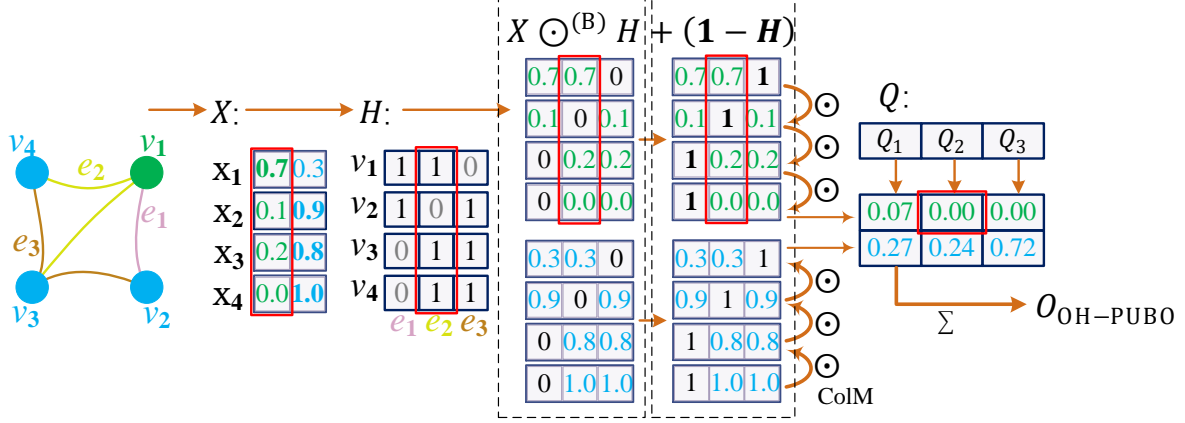


Figure 7: A toy example for Eq. 5.

where $\mathbf{x}_i \in \{0, 1\}^2$ are 2-dimensional one-hot vectors, and the matrix $[\mathbf{x}_1, \mathbf{x}_2, \dots, \mathbf{x}_{|V|}]$ is denoted by $X \in \mathbb{R}^{|V| \times 2}$. The

$$\text{OH-QUBO matrix } Q = \begin{cases} 2 & \text{if } (i, j) \in E \\ -2 & \text{if } i = j \\ 0 & \text{otherwise} \end{cases}.$$

D Proof of GPU-accelerated OH-QUBO cost function in Eq. 3

The cost function of OH-QUBO can be expressed as:

$$O_{\text{OH-QUBO}} = \sum_{i=1}^{|V|} \sum_{j=1}^{|V|} Q_{ij} \mathbf{x}_i \odot \mathbf{x}_j = \sum_{j=1}^k (x_{1j}, x_{2j}, \dots)^T Q (x_{1j}, x_{2j}, \dots) \quad (19)$$

where \mathbf{x}_i are k -dimensional one-hot vectors. $x_{ij} \in \{0, 1\}$ is the j -th element of the one-hot vector \mathbf{x}_i . Q is the OH-QUBO matrix. From Fig. 6, we can see that these two methods $O_{\text{OH-QUBO}} = \sum_{j=1}^k (x_{1j}, x_{2j}, \dots)^T Q (x_{1j}, x_{2j}, \dots)$ and $O_{\text{OH-QUBO}} = \sum X^T Q X$ (Eq. 3) are equivalent.

Note that Eq. 3 holds only if \mathbf{x}_i are discrete one-hot vectors. When relaxing $O_{\text{OH-QUBO}}$ into a differentiable loss function via softmax function, we have $\mathbf{x}_i \odot \mathbf{x}_i \neq \mathbf{x}_i$ (e.g., $0.5^2 \neq 0.5$). Thus the linear terms and quadratic terms must be handled separately as follows:

$$O_{\text{OH-QUBO}} = \sum_{\text{reduce-sum}} X^T \text{diag}(Q) + \sum_{\text{reduce-sum}} X^T (Q - \text{diag}(Q)) \odot X^T \quad (20)$$

where $\text{diag}(Q)$ denotes the diagonal matrix of Q .

E Proof of GPU-accelerated OH-PUBO cost function in Eq. 5

We present a toy example in Fig. 7 to explain the GPU-accelerated OH-PUBO cost function in Eq. 5, $O_{\text{OH-PUBO}} = \sum Q \odot^{(\text{B})} \text{ColM}(X \odot^{(\text{B})} H +^{(\text{B})} (1 - H), 1)$. As illustrated in Fig. 7, for the hypergraph $G = (V, E)$, there are four vertices v_1, v_2, v_3 and v_4 , and three hyperedges $e_1 = \{v_1, v_2\}$, $e_2 = \{v_1, v_3, v_4\}$, $e_3 = \{v_2, v_3, v_4\}$. The OH-PUBO matrix $Q = [Q_1, Q_2, Q_3]$. Thus we have $O_{\text{OH-PUBO}} = \sum (Q_1 \mathbf{x}_1 \mathbf{x}_2 + Q_2 \mathbf{x}_1 \mathbf{x}_3 \mathbf{x}_4 + Q_3 \mathbf{x}_2 \mathbf{x}_3 \mathbf{x}_4)$. Initially, we have an output of the neural network-based optimizer $X \in \mathbb{R}^{|V| \times k}$ and the incidence matrix $H \in \mathbb{R}^{|V| \times |E|}$. By using the broadcasting mechanism, we have $X \odot^{(\text{B})} H \in \mathbb{R}^{|V| \times |E| \times k}$. To perform column-wise multiplication ColM , we fill the null values with 1 by adding $(1 - H)$. Finally, we broadcast the OH-PUBO matrix Q to terms $\mathbf{x}_1 \mathbf{x}_2$, $\mathbf{x}_1 \mathbf{x}_3 \mathbf{x}_4$, and $\mathbf{x}_2 \mathbf{x}_3 \mathbf{x}_4$.

F Datasets and baseline methods

We evaluate the performance of Deep k -grouping with real-world and synthetic datasets. All publicly available and real-world graph/hypergraph datasets are summarized in Tab. 4. For synthetic datasets, we use DHG library to generate graphs and hypergraphs.

Table 4: Summary statistics of seven real-world graphs: the number of vertices $|V|$, the number of edges $|E|$. Five hypergraphs: the number of vertices $|V|$, the number of hyperedges $|E|$, the size of the hypergraph $\sum_{e \in E} |e|$.

Graphs	$ V $	$ E $	Hypergraphs	$ V $	$ E $	$\sum_{e \in E} e $
BAT	131	1,003	Primary	242	12,704	30,729
EAT	399	5,993	High	327	7,818	18,192
UAT	1,190	13,599	Cora	1,330	1,413	4,370
DBLP	2,591	3,528	Pubmed	3,824	7,523	33,687
CiteSeer	3,279	4,552	Cooking200	7,403	2,750	54,970
AmzPhoto	7,535	119,081				
AmzPc	13,471	245,861				

The baseline methods used in the experiments are summarized as below:

SCIP. A powerful open-source optimization solver that can handle mixed-integer programming (MIP) and constraint programming. In our experiment we use a SCIP optimization suit called PySCIPOpt [30], which is an interface from Python.

Tabu Search. A classic metaheuristic search method employing local search methods for combinatorial optimization. It was first formalized in 1989 [31].

GAP. The first GNN-enabled deep learning framework for graph partitioning [6]. GAP employs an end-to-end differentiable loss allowed for unsupervised training.

hMETIS. A multi-level graph and hypergraph partitioner. Well-known multi-level schemes consist of three-phases: coarsening, initial partitioning, and refinement.

KaHyPar. A modern multi-level algorithm [32] with advanced refinement techniques. It outperforms hMETIS in some cases, especially with tight imbalance constraints.